IEEE Access
Multidisciplinary | Rapid Review | Open Access Journal

SPECIAL SECTION ON WIRELESSLY POWERED NETWORKS
ALGORITHMS, APPLICATIONS AND TECHNOLOGIES

Received August 27, 2018, accepted September 19, 2018, date of publication September 28, 2018, date of current version October 19, 2018.

Digital Object Identifier 10.1109/ACCESS.2018.2872757

On Opportunistic Energy Harvesting and Information Relaying in Wireless-Powered Communication Networks

GAOFEI HUANG[1], (Member, IEEE), AND WANQING TU[2], (Senior Member, IEEE)
[1]Faculty of Mechanistic and Electric Engineering, Guangzhou University, Guangzhou 510006, China
[2]Department of Computer Science, The University of Auckland, Auckland 1142, New Zealand

Corresponding author: Gaofei Huang (huanggaofei@gzhu.edu.cn)

This work was supported in part by the National Natural Science Foundation of China under Grant 61872098, in part by the Natural Science Foundation of Guangdong Province under Grants 2017A030313363 and 2017A030310639, in part by the Science and Technology Project of Guangdong Province under Grant 2016A010101032, in part by the Featured Innovation Project of Guangdong Education Department under Grant 2016KTSCX104, and in part by the Academic Visiting Scholarship under the State Scholarship Fund of China.

ABSTRACT This paper studies a new design of a wireless-powered relay network to improve its throughput performance by opportunistic energy harvesting (EH) and information relaying (IR) at the relay node. To enable the relay to implement opportunistic EH and IR, a new protocol, namely, the adaptive harvest-store-forward (AHSF) protocol, is proposed. In the AHSF protocol, the relay is allowed to adaptively switch between an EH mode and a power-splitting (PS)-based IR mode at the beginning of each time frame; moreover, the relay can adaptively determine the amount of energy for IR based on the wireless channel conditions over one finite time horizon, which consists of multiple consecutive time frames. Then, under the proposed protocol, a throughput maximization problem is formulated to optimize the relay operation mode (i.e., EH mode or IR mode) and resource allocation (i.e., time slot, PS ratio, and power allocation) in the IR mode in a finite time horizon. The formulated problem is coupled over time and, thus, is intractable. To address the intractability, dynamic programming is employed to transform the problem into a series of Bellman equations. Based on the Bellman equations, the optimal decision criteria for the relay operation mode is derived, and a time-coupled optimization problem for the resource allocation in the IR mode is addressed by decoupling into two subproblems for two adjacent time frames. By solving the subproblems via convex programming, an optimization policy with causal channel-state information (CSI), which can be implemented online in real time, and an optimization policy with full CSI, which is used to reveal the upper bound of the achieved throughput, are achieved. The simulation results verify that the proposed design can yield significant throughput gains over the existing wireless-powered relaying schemes.

INDEX TERMS Relay, energy harvesting (EH), wireless power transfer, dynamic programming.

I. INTRODUCTION

Relay-aided transmission is a cost-efficient approach to extend wireless coverage range and thus has become a key technique in next-generation wireless networks [1]–[3]. However, in many scenarios, relay nodes are energy-constrained because they are powered only by batteries. Since the replacement of batteries may result in high cost and may even be impractical due to physical limitations (e.g., for sensors in toxic environments or inside the body) [4], [5], it is important to solve the energy scarcity problem for the relay nodes.

Wireless power transfer (WPT) [6]–[9] can provide a reliable and stable energy source for wireless nodes with the capability to harvest energy from ambient radio-frequency (RF) signals. By employing WPT in a wireless relay network, a relay node equipped with RF energy-harvesting (EH) devices can harvest energy and receive information from the RF signals emitted by the source node. Thus, WPT is promising to address the energy scarcity problem for relay nodes. As a result, a new wireless relaying communication technique, namely, wireless-powered relaying, has recently attracted intensive research interest in academia [10]–[32].

A. RELATED WORK

In the existing studies on wireless-powered relaying, the approaches for the relay to harvest energy and use the energy can be classified into two categories, namely, harvest-then-forward (HTF) and accumulate-then-forward (ATF)

approaches. In the HTF approach, the relay harvests energy and uses the harvested energy to transmit in two time slots within each time frame. Based on a power-splitting (PS) or time-switching (TS) EH receiver employed at the relay, two protocols, namely, PS-relaying (PSR) and TS-relaying (TSR) protocols, have been proposed in [10] to implement HTF relaying and have been studied for various wireless-powered relaying networks (WPRNs) in recent years. For instance, WPRNs integrating multicarrier transmission [11]–[14], multiple-input multiple-output technology [15]–[19], coherent modulated transmission with binary phase-shift keying and non-coherent modulated transmission with binary differential phase-shift keying [20], non-orthogonal multiple access [21], [22] and rateless coded transmission [23] have been studied in literature. In addition, the physical security issues in WPRNs have been investigated in [24]–[26], and a multi-relay WPRN, in which all relays assist in information relaying (IR) with a modified PSR protocol, has been studied in [27]. However, due to propagation loss, the energy harvested at the relay within one time frame can be limited, and the HTF approach potentially suffers from a low relaying capability since the amount of energy for IR is very small.

To enhance the relaying capability, the ATF approach [28]–[32], where the relay is allowed to accumulate the energy harvested in several consecutive time frames before it performs IR such that the amount of energy is sufficient to support the relay to transmit with a required power level, has been studied recently. In [28]–[30], assuming that the channel state information (CSI) is not known at the transmitter side, the ATF-based WPRNs, in which the relay forwards information with a preset fixed power level when the accumulated energy exceeds a given threshold, have been studied. In [31] and [32], an energy-threshold-based scheme, where a relay node is selected to forward information when its accumulated energy exceeds a given threshold, is employed in a WPRN with multiple relays.

B. MOTIVATIONS

Although the relaying capability is enhanced in the ATF approach, the WPRN tends to underperform in terms of throughput, which is an important performance metric for wireless networks. This underperformance occurs because the relay cannot efficiently use the harvested energy in the ATF approach, which is also a drawback of the HTF approach. Consider a scenario where the source-to-relay (SR) channel is good but the RD channel is bad due to deep fading. In this case, the amount of harvested energy at the relay is larger than that in the scenario where the SR channel is bad but the end-to-end achievable transmission rate is low due to the bad condition of the RD channel. In the worst case, where the RD channel gain is zero, the end-to-end achievable transmission rate is zero. However, if the amount of accumulated energy exceeds the given threshold, the ATF-based relay must use a given amount of energy to transmit, even though the RD channel is bad, which means that the energy is utilized inefficiently. Similarly, the same result occurs in the HTF approach since the relay must use up the harvested energy within each time frame.

On the other hand, if the relay is allowed to harvest energy in the whole time frame when the RD channel is in deep fading and is allowed to use the harvested energy to transmit in a subsequent time frame when the RD channel is improved, the energy can be utilized more efficiently and the average throughput performance over a finite time horizon that consists of multiple consecutive time frames can potentially be improved. This conclusion can be extended to more general scenarios. That is, when the SR channel condition is better than the RD channel condition, the relay should spend more resources on EH than on IR and reserve some harvested energy for IR in a subsequent time frame when the RD channel is improved. We refer to such an approach as an opportunistic EH and IR approach. Motivated by this idea, we propose a new design for the WPRN, where the relay is enabled to perform EH and IR opportunistically based on the CSI and statistics of the wireless channels in the WPRN.

C. CONTRIBUTIONS

In proposing the new design for the WPRN, our contributions in this paper can be summarized as follows.

- An important contribution of this paper is that we propose a new protocol, namely, the *adaptive harvest-store-forward (AHSF) protocol*, to enable the relay to perform EH and IR opportunistically. In the AHSF protocol, based on the knowledge of the time-varying wireless channel conditions in a finite time horizon, the relay can not only adaptively switch between the EH mode and a PSR-based IR mode at the beginning of each time frame but also adaptively determine the amount of energy used for IR. As a result, the relay can store the total harvested energy in a rechargeable battery, use all the energy for IR or separate the harvested energy into two portions, with one portion stored in the battery and the other portion used for IR.
- Another key contribution is that we propose an optimization policy that can be implemented in real time based on a look-up table, where the relay performs EH and IR opportunistically based on knowledge of the causal CSI and statistics of the wireless channels to improve the throughput for the WPRN. To achieve this goal, we formulate a throughput maximization problem under the proposed AHSF protocol to optimize the relay operation mode (i.e., EH mode or IR mode) and resource allocations (i.e., time slot, PS ratio and power allocations) in the IR mode. Because the formulated problem is coupled over time, it is intractable and hard to solve directly. To address the intractability of this problem, we employ dynamic programming to transform it into a series of Bellman equations, where the optimal decision criteria for the relay operation mode are derived and a time-coupled resource allocation problem for the IR mode is further decomposed into two subproblems for two

adjacent time frames, which can be solved by convex optimization techniques.
- Finally, our contribution also includes revealing the theoretical upper bound of the throughput performance achieved by an optimization policy with full CSI. Validated by simulations, our analysis reveals that the throughput achieved by the policy with causal CSI is much closer to the upper bound achieved by the policy with full CSI, and the proposed new design achieves significant throughput gains over the existing HTF and ATF relaying schemes.

D. ORGANIZATION

The remainder of the paper is organized as follows. Section II describes the system model, proposes the AHSF protocol and presents the throughput maximization problem. Assuming that the causal CSI and the statistics of the wireless channels are available, Section III demonstrates how to solve the formulated throughput maximization problem via dynamic programming, where an optimization policy with causal CSI is proposed. Based on the results derived in Section III, Section IV further investigates the throughput maximization problem with full CSI and presents an optimization policy to achieve the theoretical upper bound of the throughput performance. Section IV presents our simulation results to verify the optimality of the proposed optimization policy. Section V concludes the paper.

II. SYSTEM MODEL AND THE PROPOSED AHSF PROTOCOL

The WPRN studied in this paper consists of a source node (S), a destination node (D) and an EH relay node (R), and each node is equipped with one antenna. In the WPRN, we assume that a direct link between the source and destination does not exist due to physical obstacles, as has been adopted widely in the literature (e.g., [10]–[14], [18]–[20], [24], [28], [29]). As a result, a relay is necessary to assist the communication between the source and destination. Furthermore, we assume that the source has a fixed energy supply, whereas the relay is energy-constrained and equipped with a PS EH receiver and a rechargeable battery[1] to store the energy harvested from the RF signals emitted by the source. Thus, when the relay forwards the information to the destination, it can use only the harvested energy to transmit.

A. THE PROPOSED AHSF PROTOCOL

Consider one finite time horizon that consists of N consecutive time frames, and denote the index set of the N time frames as $\mathcal{N} \triangleq \{1, \cdots, N\}$. In the considered WPRN, in contrast to HTF relaying, where the relay always operates in an IR mode, we assume that the relay can operate in either an EH mode or an IR mode in each time frame. Moreover, in contrast to ATF relaying, where the relay determines its operation mode based on a given energy threshold, we assume that the relay can determine its operation mode based on a defined criterion, which is to achieve the maximum throughput over one finite time horizon. Let $\phi(n) \in \{0, 1\}$ be the indicator of the relay operation mode to be optimized later, where $\phi(n) = 0$ and $\phi(n) = 1$ indicate that the relay operates in EH mode and IR mode in time frame n, respectively.

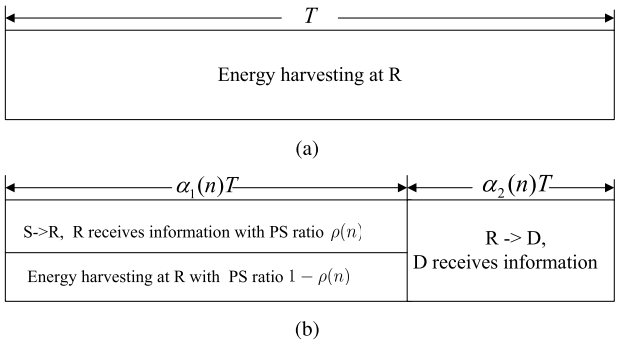

FIGURE 1. Two time frame structures for the considered WPRN. (a) The time frame structure of the EH mode. (b) The time frame structure of the PSR-based DF IR mode.

The time frame structures of the EH mode and IR mode are depicted in Figure 1, where T is the length of one time frame. As illustrated in Figure 1(a), the relay harvests energy from the RF signals emitted by the source in one complete time frame in the EH mode, and the harvested energy is stored in the rechargeable battery.

Meanwhile, as illustrated in Figure 1(b), when the relay operates in IR mode, one time frame, namely, time frame n, is divided into two time slots. We assume that the relay forwards information by decode-and-forward (DF) relaying since DF relaying outperforms amplify-and-forward (AF) relaying, and the lengths of the two time slots are denoted as $\alpha_1(n)T$ and $\alpha_2(n)T$, respectively, where $\boldsymbol{\alpha}(n) = \{\alpha_1(n), \alpha_2(n)\}$ belongs to $\mathbb{S}_\alpha(n) = \left\{\boldsymbol{\alpha}(n) \left| \sum_{i=1}^{2} \alpha_i(n) = 1, \alpha_i(n) \in [0, 1], i \in \{1, 2\} \right.\right\}$. In the first time slot, the relay uses the PS receiver to receive the RF signals transmitted by the source for information decoding (ID) and EH, where the PS ratios for ID and EH are denoted as $\rho(n) \in [0, 1]$ and $(1 - \rho(n))$, respectively. In the second time slot, the relay decodes the received information and forwards it to the destination, where the energy available for IR in time frame n is the sum of the energy stored in the battery at the beginning of time frame n and the energy harvested in the first time slot of time frame n. Furthermore, we assume that based on the time-varying wireless channel conditions over one finite time horizon, the relay can use the available energy in two ways. The first is to use all the available energy to transmit, and the second is to use a portion of the available energy to transmit and to store the remaining portion of energy in the battery.

To this end, the relay in our design can store energy after performing EH and reserve some energy in the battery while forwarding information to the destination. Moreover, the relay can adaptively determine not only its operation mode for

[1] Alternatively, a supercapacitor can be used to store the harvested energy.

each time frame but also the amount of energy to transmit in the IR mode. Therefore, we refer to this new relaying protocol as the AHSF protocol. Compared with the HTF and ATF approaches, the AHSF protocol enables the relay to perform EH and IR more flexibly, which potentially enables the relay to perform EH and IR opportunistically.

B. CHANNEL DYNAMICS AND END-TO-END ACHIEVABLE RATES

For the WPRN considered in this paper, we assume that the channels are block fading and do not vary in one time frame but vary independently in different time frames. The channel coefficients of the SR and RD links in time frame n are denoted as $h_{\mathrm{SR}}(n)$ and $h_{\mathrm{RD}}(n)$, respectively, and the corresponding channel gains are denoted as $H_{\mathrm{SR}}(n) = |h_{\mathrm{SR}}(n)|^2$ and $H_{\mathrm{RD}}(n) = |h_{\mathrm{RD}}(n)|^2$, respectively. The variances of additive white Gaussian noise (AWGN) at the receivers of the relay and the destination are denoted as σ_{R}^2 and σ_{D}^2, respectively. Furthermore, $H_{\mathrm{SR}}(n)$ and $H_{\mathrm{RD}}(n)$ are assumed to be independent of each other, and their probability density functions (pdfs) are known.

Let P_{S} be the source's transmit power, which is constant in all time frames, and let $p_{\mathrm{R}}(n)$ be the relay's transmit power in time frame n. Then, when the relay operates in IR mode, the achievable rate over the SR link can be expressed as

$$R_{\mathrm{SR}}(n) = \mathcal{C}\left(\frac{\rho(n)P_S H_{\mathrm{SR}}(n)}{\rho(n)\sigma_{\mathrm{a}}^2 + \sigma_{\mathrm{b}}^2}\right), \tag{1}$$

where $\mathcal{C}(x) = \log(1+x)$, σ_{a}^2 and σ_{b}^2 are the antenna noise power and signal processing noise power, respectively, and $\sigma_{\mathrm{a}}^2 + \sigma_{\mathrm{b}}^2 = \sigma_{\mathrm{R}}^2$. Meanwhile, the achievable rate over the RD link can be expressed as

$$R_{\mathrm{RD}}(n) = \mathcal{C}\left(\frac{p_{\mathrm{R}}(n)H_{\mathrm{RD}}(n)}{\sigma_{\mathrm{D}}^2}\right). \tag{2}$$

Thus, the end-to-end achievable rate in time frame n can be expressed as [33]

$$R(n) = \min\{\alpha_1(n)R_{\mathrm{SR}}(n), \alpha_2(n)R_{\mathrm{RD}}(n)\}. \tag{3}$$

C. EH CONSTRAINTS

Under the proposed AHSF protocol, the energy harvested in time frame n can be expressed as

$$E(n) = G(n)\left[(1-\phi(n)) + \phi(n)\alpha_1(n)(1-\rho(n))\right], \tag{4}$$

where $G(n) = \tau T P_{\mathrm{S}} H_{\mathrm{SR}}(n)$, where $0 < \tau < 1$ is the energy conversion efficiency [34].

Denote $B(1)$ as the initial energy state of the battery at the beginning of the first time frame in a finite time horizon, whose unit is joules. Since the relay can reserve some energy when it operates in IR mode and the energy used for relaying cannot exceed that stored in the battery, we have

$$\sum_{i=1}^{n} I(i) \le B(1) + \sum_{i=1}^{n} E(i), \quad \forall n \in \mathcal{N}, \tag{5}$$

where $I(n) = T\phi(n)\alpha_2(n)p_{\mathrm{R}}(n)$ denotes the energy consumed in time frame n.

Note that in practice, the capacity of a rechargeable battery is finite, and the harvested energy stored in the battery cannot exceed its capacity. Nevertheless, because the received RF power at the relay is low due to signal propagation attenuation, the amount of harvested energy cannot exceed the capacity of a battery even if the relay performs EH in N time frames over one finite time horizon.[2] Thus, we ignore the constraint on the capacity of the rechargeable battery in this paper.

III. OPTIMIZATION OF WIRELESS-POWERED RELAYING WITH CAUSAL CSI

A. PROBLEM STATEMENT

In this section, we consider the scenario where causal CSI is available. That is, before the information is transmitted at the beginning of time frame n, the transmitters of the source and the relay have knowledge only of the CSI in time frame n and the statistics of the wireless channels. We denote the CSI in time frame n as $\boldsymbol{H}(n) = \{H_{\mathrm{SR}}(n), H_{\mathrm{RD}}(n)\}$ and the network state as $\boldsymbol{s}(n) = \{\boldsymbol{H}(n), B(n)\}$.

In this paper, our goal is to maximize the throughput over one finite time horizon. Then, given $\boldsymbol{s}(1)$, considering the causality and randomness of $\boldsymbol{H}(n)$, the throughput over one finite time horizon is expressed as $\mathbb{E}\left\{\frac{1}{N}\sum_{n=1}^{N} R(n)\right\}$, where $\mathbb{E}\{\cdot\}$ is the expectation operation over all $\boldsymbol{H}(n)$s in a finite time horizon. Since the channel state $\boldsymbol{H}(1)$ and battery energy state $B(1)$ can be obtained causally prior to transmission, the throughput maximization problem for the WPRN can be expressed as

$$\max_{\pi\in\prod} \mathbb{E}\left\{\sum_{n=1}^{N} R(n)\,|\boldsymbol{s}(1)\right\} \quad \text{s.t. (5)}, \tag{6}$$

where $\pi = \{\Omega(1), \cdots, \Omega(N)\}$ is the optimization policy, in which $\Omega(n) \triangleq \{\phi(n) \in \{0,1\}, p_{\mathrm{R}}(n) \ge 0, \boldsymbol{\alpha}(n) \in \mathbb{S}_{\alpha}(n), \rho(n) \in [0,1]\}$ is the variable set to be optimized and defined as the decision for time frame n, and $\prod$ is the space of all involved feasible policies. Note that except for $\phi(n)$, all the variables in $\Omega(n)$ are for the resource allocations in IR mode.

B. REWRITING THE EH CONSTRAINT BY INTRODUCING AUXILIARY BATTERY ENERGY STATES

Because problem (6) is coupled over time, it is intractable and cannot be solved directly. To overcome the intractability of the EH constraint in problem (6), we let the energy state of the battery at time frame n^-, which denotes the instant at the beginning of time frame n, be $B(n)$. Practically, $B(n)$ is continuous. However, to make the optimization problem tractable, we assume that $B(n)$ is discrete, i.e., $B(n) \in \mathcal{B}$, with $\mathcal{B} \triangleq \left\{m\frac{B_{\mathrm{s}}}{M}, m = 0, 1, \cdots, M\right\}$, where B_{s} denotes the maximum amount of harvested energy stored in the battery.

[2] As illustrated in Figure 5(b), the amount of energy that must be stored in the battery is no more than 100 nanojoules.

When M is sufficiently large, the discretized energy state model approaches the continuous one [35]. We further introduce an auxiliary battery energy state $B(n+1)$, which refers to the battery energy sate at time frame $(n+1)^-$. Note that $B(n)$ can be acquired by the relay prior to the transmission of time frame n; however, since the decision $\Omega(n)$ is not known, $B(n+1)$ is a variable to be optimized that must satisfy

$$B(n+1) \in \mathcal{B}, \quad \forall n \in \mathcal{N}^-, \tag{7}$$

where $\mathcal{N}^- \triangleq \{1, \cdots, N-1\}$. Then, given $B(n)$, the EH constraint in (5) can be rewritten as

$$I(n) \leq B(n) + E(n) - B(n+1), \quad \forall n \in \mathcal{N}^-. \tag{8}$$

Furthermore, to ensure that the inequality (8) is satisfied, the right-hand side of (8) should be nonnegative, i.e.,

$$B(n) + E(n) - B(n+1) \geq 0, \tag{9}$$

for any $E(n)$. According to (4), we have $E(n) \leq G(n)$. Thus, according to (9), $B(n+1)$ should satisfy

$$B(n+1) \leq B(n) + G(n). \tag{10}$$

To achieve maximum throughput, the relay always operates in IR mode and consumes all the available energy to transmit in time frame N. Thus, for $n = N$, the EH constraint in (5) can be rewritten as

$$I(N) \leq B(N) + E(N). \tag{11}$$

Define the battery energy state subset that satisfies (7) and (10) as $\mathcal{B}'$. Then, after introducing the auxiliary variable $B(n+1)$, the optimization variable set for $n \in \mathcal{N}^-$ can be rewritten as $\Omega'(n) = \Omega(n) \bigcup \{B(n+1) \in \mathcal{B}'\}$. Meanwhile, the optimization variable set for time frame N remains $\Omega(N)$.

C. DECOUPLING PROBLEM BY DYNAMIC PROGRAMMING

Based on the rewritten EH constraints in (8) and (11), problem (6) can be transformed into a series of Bellman equations by employing the dynamic programming technique [38]. That is, given $\boldsymbol{s}(1)$, problem (6) can be solved by proceeding backward in time from time frame N to time frame 1 to solve the following Bellman equations,

$$J^*(\boldsymbol{s}(N), N) = \max_{\Omega(N)} \phi(N) R(N) \quad \text{s.t. (11)}, \tag{12}$$

and

$$J^*(\boldsymbol{s}(n), n) = \max_{\Omega'(n)} \phi(n) R(n) + \overline{J}^*(\boldsymbol{s}(n+1), (n+1)) \quad \text{s.t. (8)}, \tag{13}$$

where $n \in \mathcal{N}^-$ and

$$\overline{J}^*(\boldsymbol{s}(n+1), (n+1)) = \mathbb{E}_{\boldsymbol{H}(n+1)}\left[J^*(\boldsymbol{s}(n+1), (n+1))\right]. \tag{14}$$

Although the optimization policy can be obtained by solving the Bellman equations in (12) and (13), these Bellman equations are difficult to solve for two reasons. First, $\overline{J}^*(\boldsymbol{s}(n+1), (n+1))$ in (14) is not easy to obtain, even though the pdf of $\boldsymbol{H}(n+1)$ is known. Second, the problem in (13) is still time-coupled since $\Omega(n)$ and $B(n+1)$, which are for time frame n and time frame $n+1$, respectively, are included in $\Omega'(n)$. To overcome these difficulties, we adopt a finite-state Markov channel model with the equiprobable steady state [36], which has been widely used for modeling wireless flat-fading channels, to represent the CSI $\boldsymbol{H}(n)$. Assume that the number of finite states is K. Let $\chi_{\mathrm{SR}}(n)$ and $\chi_{\mathrm{RD}}(n)$ be the quantized channel gains for $H_{\mathrm{SR}}(n)$ and $H_{\mathrm{RD}}(n)$, respectively. Denote $\boldsymbol{\chi}(n) = \{\chi_{\mathrm{SR}}(n), \chi_{\mathrm{RD}}(n)\}$ as the channel state for $\boldsymbol{H}(n)$, and define the corresponding network state as $\boldsymbol{\Gamma}(n) = \{\boldsymbol{\chi}(n), B(n)\}$. Then, by replacing $\boldsymbol{s}(n)$ with $\boldsymbol{\Gamma}(n)$ and replacing $\boldsymbol{H}(n)$ with $\boldsymbol{\chi}(n)$, the Bellman equations in (12) and (13) can be rewritten as

$$J^*(\boldsymbol{\Gamma}(N), N) = \max_{\Omega(N)} \phi(N) \hat{R}(N) \quad \text{s.t. } I(N) \leq B(N) + \hat{E}(N) \tag{15}$$

and

$$J^*(\boldsymbol{\Gamma}(n), n) = \max_{\Omega'(n)} \phi(n) \hat{R}(n) + \overline{J}^*(\boldsymbol{\Gamma}(n+1), (n+1)) \quad \text{s.t. } I(n) \leq B(n) + \hat{E}(n) - B(n+1), \tag{16}$$

respectively, where $\hat{R}(n)$ is obtained by replacing $\boldsymbol{H}(n)$ with $\boldsymbol{\chi}(n)$ in $R(n)$, and $\hat{E}(n)$ is obtained by replacing $\boldsymbol{H}(n)$ with $\boldsymbol{\chi}(n)$ in $E(n)$.

As the K-state Markov channel model with the equiprobable steady state is adopted, $\overline{J}^*(\boldsymbol{\Gamma}(n+1), (n+1))$ in (14) can be expressed as

$$\begin{aligned} &\overline{J}^*(\boldsymbol{\Gamma}(n+1), (n+1)) \\ &= \sum_{\boldsymbol{\chi}(n+1)} \left[p(\boldsymbol{\chi}(n+1)) J^*(\boldsymbol{\Gamma}(n+1), (n+1))\right] \\ &= \frac{1}{K^2} \sum_{\boldsymbol{\chi}(n+1)} \left[J^*(\boldsymbol{\Gamma}(n+1), (n+1))\right], \end{aligned} \tag{17}$$

where $p(\boldsymbol{\chi}(n+1)) = \frac{1}{K^2}$ is the probability of $\boldsymbol{\chi}(n+1)$.

Then, by solving the Bellman equations in (15) and (16), a look-up table can be constructed offline, and the optimization policy can be achieved based on the look-up table. The details will be presented after the solutions to the Bellman equations in (15) and (16) are derived. In the following, we focus on how to solve these Bellman equations. To achieve this goal, we first obtain the solution of $\phi(n)$ to determine the optimal relay operation mode and then derive the solutions of the other variables in $\Omega'(n)$, which include the auxiliary energy state $B(n+1)$ and the variables for the resource allocation in IR mode.

For simplicity, we derive the solutions to the Bellman equations in (15) and (16) by solving the Bellman equations in (12) and (13) since they have the same structures and the solutions have the same forms.

D. OPTIMAL RELAY OPERATION MODE

As mentioned previously, the relay is bound to operate in IR mode in time frame N to achieve the maximum throughput over one finite time horizon. Thus, the optimal solution of $\phi(N)$ to problem (12) is $\phi^*(N) = 1$.

For $n \in \mathcal{N}^-$, when the relay operates in EH mode in time frame n, we have $B(n+1) = B(n) + G(n)$. Since the battery energy states are discrete, $B(n+1)$ can be expressed as

$$\tilde{B}(n+1) = \arg\min_{b \in \mathcal{B}} B(n) + G(n) - b, \quad \text{s.t. } B(n) + G(n) \geq b. \tag{18}$$

Let $\tilde{\boldsymbol{s}}(n+1) = \left\{\boldsymbol{H}(n+1), \tilde{B}(n+1)\right\}$. Then, we have the following theorem for the optimal relay operation mode.

Theorem 1: The optimal $\phi^*(n)$ to problem (13) can be obtained as

$$\phi^*(n) = \begin{cases} 0, & J_0^*(\boldsymbol{s}(n), n) \geq J_1^*(\boldsymbol{s}(n), n) \\ 1, & \text{otherwise}, \end{cases} \tag{19}$$

where

$$J_0^*(\boldsymbol{s}(n), n) = \overline{J}^*\left(\tilde{\boldsymbol{s}}(n+1), (n+1)\right) \tag{20}$$

and

$$J_1^*(\boldsymbol{s}(n), n) = \max_{\Omega''(n)} R(n) + \overline{J}^*\left(\boldsymbol{s}(n+1), (n+1)\right) \tag{21a}$$

$$\text{s.t. } I'(n) \leq B(n) + E'(n) - B(n+1) \tag{21b}$$

with $\Omega''(n) = \Omega'(n) \backslash \phi(n)$, $I'(n) = T\alpha_2(n) p_{\mathrm{R}}(n)$ and $E'(n) = \alpha_1(n) G(n)[1 - \rho(n)]$.

Proof: Please refer to Appendix A. ■

Remark 1: According to (18), the larger $H_{\mathrm{SR}}(n)$ is, the larger $\tilde{B}(n+1)$ is. Meanwhile, according to (13), $J_1^*(\boldsymbol{s}(n), n)$ is a monotone increasing function of $B(n)$. Thus, the larger $H_{\mathrm{SR}}(n)$ is, the larger $J^*\left(\tilde{\boldsymbol{s}}(n+1), (n+1)\right)$ is, which results in a larger $J_0^*(\boldsymbol{s}(n), n)$. Meanwhile, the smaller $H_{\mathrm{RD}}(n)$ is, the smaller the achievable rate over the relay link is, which results in a smaller $J_1^*(\boldsymbol{s}(n), n)$. Therefore, as $H_{\mathrm{SR}}(n)$ increases and $H_{\mathrm{RD}}(n)$ decreases, the relay become more likely to operate in EH mode since $J_1^*(\boldsymbol{s}(n), n)$ is more likely to be smaller than $J_0^*(\boldsymbol{s}(n), n)$. Thus, the relay prefers to perform EH in the scenario where the SR channel is good and the RD channel is bad, which indicates that it operates in EH mode in an opportunistic manner.

In Theorem 1, we focus only on how to calculate $J_1^*(\boldsymbol{s}(n), n)$ by solving problem (21). This problem corresponds to optimizing the auxiliary energy state and the resource allocation in IR mode, which will be discussed in the following subsection.

E. OPTIMIZATION OF THE AUXILIARY ENERGY STATE AND THE RESOURCE ALLOCATION IN IR MODE

Because $B(n+1)$ is included in $\Omega''(n)$, problem (21) is coupled over two adjacent time frames. Thus, problem (21) remains difficult to solve directly. To address this problem, we decompose it into two subproblems. The first subproblem is to optimize the resource allocation in time frame n for any given $B(n+1) \in \mathcal{B}'$, where the optimal value is denoted as

$$F^*(B(n+1)) = \max_{\bar{\Omega}(n)} R(n) \text{ s.t. (21b)}, \tag{22}$$

in which $\bar{\Omega}(n) = \Omega''(n) \backslash B(n+1)$. The second subproblem is to obtain the optimal $B^*(n+1)$, which is stated as

$$J_1^*(\boldsymbol{s}(n), n) = \max_{B(n+1) \in \mathcal{B}'} F^*(B(n+1)) + \overline{J}^*\left(\boldsymbol{s}(n+1), (n+1)\right). \tag{23}$$

When $F^*(B(n+1))$ is achieved, problem (23) can be solved by exhaustively searching for the optimal $B^*(n+1)$ in $\mathcal{B}'$. Therefore, we need to focus only on solving problem (22).

According to (3), $R(n)$ is non-concave. Moreover, the EH constraint (21b) is non-convex. Thus, problem (22) is non-convex. Although a similar optimization problem for the PSR-based DF WPRN with HTF relaying has been recently studied [23], the optimization method provided in [23] cannot be employed to solve problem (22) because in the PSR-based DF WPRN with HTF relaying, the initial energy state at the relay's battery at the beginning of each time frame is zero. Thus, the transmit power at the relay can be expressed by the time slot and PS ratios in a simplified form. This simplified form can be used to derive the optimal time slot and PS ratios by means of a series of algebraic manipulations, as illustrated in [23]. However, due to the non-zero term $(B(n) - B(n+1))$ in (21b), the optimal time slot and PS ratios cannot be derived by the method provided in [23]. Therefore, the optimal solution to problem (22) is non-trivial to obtain.

To solve problem (22), as in [37], we assume that power splitting reduces only the signal power and not the noise power. Then, $R_{\mathrm{SR}}(n)$ in (1) can be simplified as $R_{\mathrm{SR}}(n) \approx \mathcal{C}\left(\frac{\rho(n) P_S H_{\mathrm{SR}}(n)}{\sigma_{\mathrm{R}}^2}\right)$, by which a lower bound of $R_{\mathrm{SR}}(n)$ is obtained. Moreover, let $\omega(n) = \alpha_1(n)\rho(n)$ and $\widetilde{p}_{\mathrm{R}}(n) = \alpha_2(n) p_{\mathrm{R}}(n)$. Then, the expression of $R(n)$ in (3) can be expressed as

$$R'(n) = \min\left\{\alpha_1(n) R'_{\mathrm{SR}}(n), \alpha_2(n) R'_{\mathrm{RD}}(n)\right\}, \tag{24}$$

where $R'_{\mathrm{SR}}(n) = \mathcal{C}\left(\frac{\omega(n)}{\alpha_1(n)} \frac{P_S H_{\mathrm{SR}}(n)}{\sigma_{\mathrm{R}}^2}\right)$ and $R'_{\mathrm{RD}}(n) = \mathcal{C}\left(\frac{\widetilde{p}_{\mathrm{R}}(n)}{\alpha_2(n)} \frac{H_{\mathrm{RD}}(n)}{\sigma_{\mathrm{D}}^2}\right)$, and the problem in (22) can be rewritten as

$$\max_{\bar{\Omega}'(n)} R'(n) \tag{25a}$$

$$\text{s.t. } T\widetilde{p}_{\mathrm{R}}(n) \leq B(n) + E''(n) - B(n+1), \tag{25b}$$

$$\omega(n) \leq \alpha_1(n), \tag{25c}$$

where $\bar{\Omega}'(n) \triangleq \{\widetilde{p}_{\mathrm{R}}(n) \geq 0, \omega(n) \geq 0, \boldsymbol{\alpha}(n) \in \mathbb{S}_\alpha(n)\}$ and $E''(n) = G(n)[\alpha_1(n) - \omega(n)]$. Problem (25) can be proved to be convex. To this end, problem (25) can be solved by optimization software, e.g., CVX [40]. Nevertheless, to gain insight into the resource allocation, we derive the analytical solution to problem (25) in the following.

Since $\alpha_2(n) = 1-\alpha_1(n)$, the optimal value of problem (25) can be obtained by

$$\max_{\alpha_1(n)\in[0,1]} Q^*(\alpha_1(n)), \tag{26}$$

where $Q^*(\alpha_1(n))$ is the optimal value of problem (25) for any fixed $\alpha_1(n)$, i.e.,

$$\begin{aligned} Q^*(\alpha_1(n)) = \max_{\bar{\Omega}'(n)}\ & u(n) && \text{(27a)}\\ \text{s.t. (25b)},\ & \omega(n) \le \alpha_1(n), && \text{(27b)}\\ & u(n) \le \alpha_1(n)R'_{\mathrm{SR}}(n),\ u(n) \le \alpha_2(n)R'_{\mathrm{RD}}(n) && \text{(27c)} \end{aligned}$$

with $\bar{\Omega}'(n) \triangleq \{u(n), \widetilde{p}_{\mathrm{R}}(n) \ge 0, \omega(n) \ge 0\}$. Therefore, we first solve problem (27) for any fixed $\alpha_1(n)$ and then solve problem (26) to achieve the optimal $\alpha_1^*(n)$, by which the optimal $\alpha_2^*(n)$ can be obtained.

To solve problem (27), we construct the Lagrangian as

$$\begin{aligned} &\mathcal{L}(\Theta(n))\\ &= u(n) - \lambda_1(n)\left[T\widetilde{p}_{\mathrm{R}}(n) - B(n) - E''(n) + B(n+1)\right]\\ &\quad - \lambda_2(n)\left[\omega(n) - \alpha_1(n)\right] - \upsilon_1(n)\left[u(n) - \alpha_1(n)R'_{\mathrm{SR}}(n)\right]\\ &\quad - \upsilon_2(n)\left[u(n) - \alpha_2(n)R'_{\mathrm{RD}}(n)\right], \end{aligned} \tag{28}$$

where $\Theta(n) = \{\boldsymbol{\lambda}(n), \boldsymbol{\upsilon}(n)\} \bigcup \bar{\Omega}'(n)$, in which $\boldsymbol{\lambda}(n) = [\lambda_1(n), \lambda_2(n)] \succeq 0$ and $\boldsymbol{\upsilon}(n) = [\upsilon_1(n), \upsilon_2(n)] \succeq 0$ denote the Lagrangian multipliers. Then, the dual objective function is

$$g(\boldsymbol{\lambda}(n), \boldsymbol{\upsilon}(n)) = \max_{\bar{\Omega}'(n)} \mathcal{L}(\Theta(n)), \tag{29}$$

and the dual problem is

$$\begin{aligned} \min_{\boldsymbol{\lambda}(n),\boldsymbol{\upsilon}(n)}\ & g(\boldsymbol{\lambda}(n), \boldsymbol{\upsilon}(n)) && \text{(30a)}\\ \text{s.t. } & \lambda_i(n) \ge 0, \quad \upsilon_i(n) \ge 0,\ \forall i = \{1, 2\}. && \text{(30b)} \end{aligned}$$

According to the Karush-Kuhn-Tucker (KKT) conditions [39], given any dual variables $(\boldsymbol{\lambda}(n), \boldsymbol{\upsilon}(n))$, the optimal $\omega^*(n)$ and $\widetilde{p}_{\mathrm{R}}^*(n)$ must satisfy

$$\begin{aligned} \frac{\partial \mathcal{L}(\Theta(n))}{\partial \omega(n)} &= \frac{\upsilon_1(n)\alpha_1(n)P_S\gamma_{\mathrm{SR}}(n)}{\alpha_1(n) + \omega^*(n)P_S\gamma_{\mathrm{SR}}(n)} - \lambda_1(n)G(n)\\ &\quad - \lambda_2(n)\begin{cases} \ge 0, & \text{if } \omega^*(n) = 0;\\ = 0, & \text{if } \omega^*(n) > 0, \end{cases} \end{aligned} \tag{31}$$

$$\begin{aligned} \frac{\partial \mathcal{L}(\Theta(n))}{\partial \widetilde{p}_{\mathrm{R}}(n)} &= -\lambda_1(n)T + \frac{\upsilon_2(n)\alpha_2(n)\gamma_{\mathrm{RD}}(n)}{\alpha_2(n) + \widetilde{p}_{\mathrm{R}}^*(n)\gamma_{\mathrm{RD}}(n)}\\ &\quad \times \begin{cases} \ge 0, & \text{if } \widetilde{p}_{\mathrm{R}}^*(n) = 0;\\ = 0, & \text{if } \widetilde{p}_{\mathrm{R}}^*(n) > 0, \end{cases} \end{aligned} \tag{32}$$

where $\gamma_{\mathrm{SR}}(n) = \frac{H_{\mathrm{SR}}(n)}{\sigma_{\mathrm{R}}^2}$ and $\gamma_{\mathrm{RD}}(n) = \frac{H_{\mathrm{RD}}(n)}{\sigma_{\mathrm{D}}^2}$.

Moreover, according to the complementary slackness condition [39], we have $\lambda_2(n)\left[\omega^*(n) - \alpha_1(n)\right] = 0$. Thus, to obtain the optimal $\omega^*(n)$ and $\widetilde{p}_{\mathrm{R}}^*(n)$, we investigate the following two cases.

Case 1 ($\omega^*(n) < \alpha_1(n)$): In this case, we obtain $\lambda_2(n) = 0$. Thus, by (31) and (32), we obtain

$$\omega^*(n) = \alpha_1(n)\left[\frac{\upsilon_1(n)}{\lambda_1(n)G(n)} - \frac{1}{P_S\gamma_{\mathrm{SR}}(n)}\right]^+ \tag{33}$$

$$\widetilde{p}_{\mathrm{R}}^*(n) = \alpha_2(n)\left[\frac{\upsilon_2(n)}{\lambda_1(n)T} - \frac{1}{\gamma_{\mathrm{RD}}(n)}\right]^+, \tag{34}$$

where $[x]^+ \triangleq \max(0, x)$.

Furthermore, to obtain the optimal $\left(\lambda_1^*(n), \boldsymbol{\upsilon}^*(n)\right)$, we observe that $\boldsymbol{\upsilon}^*(n)$ should satisfy

$$\frac{\partial \mathcal{L}(\Theta(n))}{\partial u(n)} = 1 - \left[\upsilon_1^*(n) + \upsilon_2^*(n)\right] = 0. \tag{35}$$

Thus, we can obtain the tuples $\left(\lambda_1^*(n), \upsilon_1^*(n)\right)$ by two-level bisection searching over the two-dimensional dual set $\Lambda = \left\{(\lambda_1(n), \upsilon_1(n)) | \lambda_{1,\min} \le \lambda_1(n) \le \lambda_{1,\max}, 0 \le \upsilon_1(n) \le \upsilon_{1,\max}\right\}$, where $\lambda_{1,\min} = \frac{P_S\gamma_{\mathrm{SR}}(n)\upsilon_1(n)}{(1+P_S\gamma_{\mathrm{SR}}(n))G(n)}$, $\lambda_{1,\max} = \frac{\gamma_{\mathrm{RD}}(n)(1-\upsilon_1(n))}{T}$ and $\upsilon_{1,\max} = \frac{\zeta}{P_S\gamma_{\mathrm{SR}}(n)+\zeta}$, with $\zeta = (1 + P_S\gamma_{\mathrm{SR}}(n))G(n)\gamma_{\mathrm{RD}}(n)/T$, as derived in Appendix B.

Based on the optimal $Q^*(\alpha_1(n))$, we can solve problem (26) by the golden section method to obtain $\alpha_1^*(n)$ since the objective function in problem (26) is concave in $\alpha_1(n)$.

Then, the corresponding algorithm to solve problem (25) in the case of $\omega^*(n) < \alpha_1(n)$ is illustrated in Algorithm 1.

Algorithm 1 Optimization Algorithm to Solve Problem (25) in the Case of $\omega^*(n) < \alpha_1(n)$

1: **Initialization:** Set tolerance $\epsilon_\alpha > 0$, $\alpha_1^{\min} = 0$, $\alpha_1^{\max} = 1$, $\alpha_1^{\mathrm{U}} = \alpha_1^{\max}$ and $\alpha_1^{\mathrm{L}} = \alpha_1^{\min}$.
2: **while** $\alpha_1^{\mathrm{U}} - \alpha_1^{\mathrm{L}} > \epsilon_\alpha$ **do**
3: $\quad \alpha_1^{\mathrm{U}} = \alpha_1^{\min} + (\alpha_1^{\max} - \alpha_1^{\min}) * 0.618$,
4: $\quad \alpha_1^{\mathrm{L}} = \alpha_1^{\max} + \alpha_1^{\min} - \alpha_1^{\mathrm{U}}$,
5: $\quad$ Use $\alpha_1(n) = \alpha_{\mathrm{U}}$ and $\alpha_1(n) = \alpha_{\mathrm{L}}$ to calculate the optimal $\left(\bar{\Omega}'^*(n), Q^*(\alpha_1(n))\right)$ to problem (27) to obtain $\left(\bar{\Omega}_{\mathrm{U}}'^*(\alpha_1(n)), Q_{\mathrm{U}}^*(\alpha_1(n))\right)$ and $\left(\bar{\Omega}_{\mathrm{L}}'^*(\alpha_1(n)), Q_{\mathrm{L}}^*(\alpha_1(n))\right)$, respectively,
6: $\quad$ **if** $Q_{\mathrm{U}}^*(\alpha_1(n)) > Q_{\mathrm{L}}^*(\alpha_1(n))$ **then**
7: $\quad\quad \alpha_1^{\min} = \alpha_1^{\mathrm{L}}$,
8: $\quad$ **else**
9: $\quad\quad \alpha_1^{\max} = \alpha_1^{\mathrm{U}}$.
10: $\quad$ **end if**
11: **end while**
12: Use $\alpha_1^*(n) = (\alpha_1^{\mathrm{U}} + \alpha_1^{\mathrm{L}})/2$ to obtain the optimal value of (25) and use $\bar{\Omega}_{\mathrm{U}}'^*(\alpha_1(n))$ (or $\bar{\Omega}_{\mathrm{L}}'^*(\alpha_1(n))$) to obtain the optimal $\bar{\Omega}'^*(n)$ to problem (25) with $\omega^*(n) < \alpha_1(n)$.

Case 2 $\omega^*(n) = \alpha_1(n)$: In this case, the optimal $\rho^*(n)$ to problem (22) is $\rho^*(n) = 1$. Moreover, problem (27) can be rewritten as

$$\begin{aligned} Q^*(\alpha_1(n)) = \max_{\bar{\Omega}''(n)}\ & u(n) && \text{(36a)}\\ \text{s.t. } & T\widetilde{p}_{\mathrm{R}}(n) \le B(n) - B(n+1), && \text{(36b)} \end{aligned}$$

$$u(n) \le \alpha_1(n) R''_{\mathrm{SR}}(n),$$
$$u(n) \le \alpha_2(n) R'_{\mathrm{RD}}(n), \tag{36c}$$

where $\bar{\Omega}''(n) \triangleq \{u(n), \widetilde{p}_{\mathrm{R}}(n) \ge 0\}$ and $R''_{\mathrm{SR}}(n) = \mathcal{C}(P_S \gamma_{\mathrm{SR}}(n))$.

Note that given $B(n+1)$, there may be $B(n) - B(n+1) < 0$ for $B(n+1) \in \mathcal{B}'$. Thus, if $B(n) - B(n+1) < 0$ for the given $B(n+1)$, the EH constraint (36b) cannot be satisfied, and there is no feasible solution to problem (36). In this case, we let $\widetilde{p}^*_{\mathrm{R}}(n) = 0$. Otherwise, according to problem (36) and problem (26), we have the following problem, which is to solve problem (25) in the case of $\omega^*(n) = \alpha_1(n)$,

$$\max_{\bar{\Omega}'''(n)} \min\left\{\alpha_1(n) R''_{\mathrm{SR}}(n), \alpha_2(n) R'_{\mathrm{RD}}(n)\right\} \quad \text{s.t. (36b)}, \tag{37}$$

where $\bar{\Omega}'''(n) \triangleq \{\widetilde{p}_{\mathrm{R}}(n) \ge 0, \boldsymbol{\alpha}(n) \in \mathbb{S}_\alpha(n)\}$.

Since $\widetilde{p}_{\mathrm{R}}(n) = \alpha_2(n) p_{\mathrm{R}}(n)$, problem (37) can also be expressed as

$$\max_{\Omega'''(n)} \min\left\{\alpha_1(n) R''_{\mathrm{SR}}(n), \alpha_2(n) R_{\mathrm{RD}}(n)\right\} \tag{38a}$$
$$\text{s.t. } T\alpha_2(n) p_{\mathrm{R}}(n) \le B(n) - B(n+1), \tag{38b}$$

where $\Omega'''(n) \triangleq \{p_{\mathrm{R}}(n) \ge 0, \boldsymbol{\alpha}(n) \in \mathbb{S}_\alpha(n)\}$. Then, to solve problem (38), we have the following lemma.

Lemma 1: The optimal solution of $\Omega'''(n)$ to problem (38) should satisfy

$$\alpha_1(n) R''_{\mathrm{SR}}(n) \ge \alpha_2(n) R_{\mathrm{RD}}(n). \tag{39}$$

Proof: Please refer to Appendix C. ■

We have the following theorem based on Lemma 1.

Theorem 2: When $B(n) - B(n+1) \ge 0$, the optimal solution $\Omega'''(n)$ to problem (38) should satisfy that the EH constraint (38b) is active, i.e.,

$$T\alpha_2(n) p_{\mathrm{R}}(n) = B(n) - B(n+1). \tag{40}$$

Proof: Please refer to Appendix D. ■

Then, the optimal solution of $p_{\mathrm{R}}(n)$ to problem (38) should satisfy

$$\bar{p}_{\mathrm{R}}(n) = \left[\frac{B(n) - B(n+1)}{T\alpha_2(n)}\right]^+, \tag{41}$$

and problem (38) can be rewritten as

$$\max_{\boldsymbol{\alpha}(n) \in \mathbb{S}_\alpha(n)} \min\left\{\alpha_1(n) R''_{\mathrm{SR}}(n), \alpha_2(n) R''_{\mathrm{RD}}(n)\right\}, \tag{42}$$

where $R''_{\mathrm{RD}}(n) = \mathcal{C}(\bar{p}_{\mathrm{R}}(n) \gamma_{\mathrm{RD}}(n))$.

The objective function in problem (42) can be proved to be concave. Thus, we can obtain the optimal $\boldsymbol{\alpha}^*(n)$ to problem (42) by using the golden section method.

Summarizing the results in **Case 1** and **Case 2**, we can solve problem (22) to optimize the resource allocations in IR mode by Algorithm 2.

Finally, according to (12), the optimization problem for the resource allocations in IR mode in time frame N can be expressed as

$$J^*(\boldsymbol{s}(N), N) = \max_{\bar{\Omega}(N)} R(N) \quad \text{s.t. (11)}, \tag{43}$$

Algorithm 2 Optimization Algorithm to Solve Problem (22)

1: Calculate the optimal value and the optimal solution to problem (25) by Algorithm 1, which are denoted as Z_1 and $\bar{\Omega}'^*_1(n)$, respectively.
2: Solve problem (42) by the golden section method to obtain the optimal value and the optimal solution to problem (22), which are denoted as Z_2 and $\bar{\Omega}^*_2(n)$, respectively.
3: **if** $Z_1 \ge Z_2$ **then**
4: Obtain the optimal $F^*(B(n+1)) = Z_1$ and derive $\bar{\Omega}^*(n)$ by $\bar{\Omega}'^*_1(n)$.
5: **else**
6: Obtain $F^*(B(n+1)) = Z_2$ and $\bar{\Omega}^*(n) = \bar{\Omega}^*_2(n)$.
7: **end if**

where $\bar{\Omega}(N) \triangleq \{p_{\mathrm{R}}(N) \ge 0, \boldsymbol{\alpha}(N) \in \mathbb{S}_\alpha(N), \rho(N) \in [0, 1]\}$. It is easy to verify that problem (43) can also be solved by Algorithm 2.

Remark 2: In **Case 1**, (33) can be rewritten as $\rho^*(n) = \frac{1}{H_{\mathrm{SR}}(n)}\left[\frac{\upsilon_1(n)}{\lambda_1(n)\tau T P_S} - \frac{1}{P_S/\sigma^2_{\mathrm{R}}(n)}\right]^+$. Then, the larger the SR channel gain is, the more energy is used for EH. Therefore, in this case, the relay also harvests energy in an opportunistic manner in IR mode, which is similar to that in EH mode, since it prefers to perform EH rather than ID when the SR channel condition is good. Meanwhile, according to (34), the larger the RD channel gain is, the larger the relay's transmit power is, which indicates that the relay performs IR opportunistically since its transmit power is larger when the RD channel is better. In **Case 2**, $\rho^*(n) = 1$ means that the relay does not harvest any energy. Moreover, according to (41), the relay determines its transmit power based only on the battery energy states (i.e., $B(n)$ and $B(n+1)$) and does not take the CSI into account. This scenario occurs only when the amount of energy stored in the battery is large, such that $Z_1 < Z_2$ is satisfied in Algorithm 2.

F. ALGORITHM TO ACHIEVE THE OPTIMIZATION POLICY WITH CAUSAL CSI

After obtaining the solution to the Bellman equation (12) and (13), the optimization policy with causal CSI can be obtained in two steps. First, based on the K-state Markov channel model, a look-up table can be constructed offline before transmission. The look-up table contains $(N-1) \times K^2 \times (M+1)$ entries, and one entry corresponds to one state $\boldsymbol{\Gamma}(n)$, where $n \in \mathcal{N}^-$. In the entry corresponding to $\boldsymbol{\Gamma}(n)$, $\{\phi^*(n), \bar{B}^*(n+1)\}$ is recorded, where $\bar{B}^*(n+1) = B^*(n+1)$ (i.e., the optimal solution to problem (23)) for $\phi^*(n) = 1$ and $\bar{B}^*(n+1) = \emptyset$ (i.e., null) for $\phi^*(n) = 0$. Note that $\bar{B}^*(n+1)$ is set to $\emptyset$ for $\phi^*(n) = 0$ because $B(n+1)$ is not required to obtain the decision for time frame n when the relay operates in EH mode. The corresponding algorithm to construct the look-up table is illustrated in Algorithm 3, where $\mathbb{X}$ is the set of all possible quantized channel states (i.e., $\boldsymbol{\chi}(n)$'s).

Algorithm 3 Construction of the Look-Up Table for the Optimization Policy With Causal CSI

Initialize $\mathbb{X}$ and the set of battery energy states $B(n) \in \mathcal{B}$, $\forall n \in \mathcal{N}$.
for all possible $B(N) \in \mathcal{B}$ **do**
  for all possible $\boldsymbol{\chi}(N) \in \mathbb{X}$ **do**
    Let $\phi^*(N) = 1$ and solve problem (43) to obtain $J^*(\boldsymbol{\Gamma}(N), N)$.
  end for
  Calculate $\overline{J}^*(\boldsymbol{\Gamma}(N), N)$ by (17).
end for
Set $n = N$.
Repeat:
Update $n = n - 1$.
for all possible $B(n) \in \mathcal{B}$ **do**
  for all possible $\boldsymbol{\chi}(n) \in \mathbb{X}$, **do**
    Calculate $J_0^*(\boldsymbol{\Gamma}(n), n)$ by (20), solve problem (22) and (23) to obtain $J_1^*(\boldsymbol{\Gamma}(n), n)$ and $B^*(n+1)$, determine the optimal $\phi^*(n)$ by (19).
    if $\phi^*(n) = 0$ **then**
      Let $J^*(\boldsymbol{\Gamma}(n), n) = J_0^*(\boldsymbol{\Gamma}(n), n)$,
      Record $\left\{\phi^*(n) = 0, \bar{B}^*(n+1) = \emptyset\right\}$ in the entry corresponding to $\boldsymbol{\Gamma}(n)$.
    else
      Let $J^*(\boldsymbol{\Gamma}(n), n) = J_1^*(\boldsymbol{\Gamma}(n), n)$,
      Record $\left\{\phi^*(n) = 1, \bar{B}^*(n+1) = B^*(n+1)\right\}$ in the entry corresponding to $\boldsymbol{\Gamma}(n)$.
    end if
  end for
  if $n > 1$ **then**
    Calculate $\overline{J}^*(\boldsymbol{\Gamma}(n), n)$ by (17).
  end if
end for
Until: $n = 1$.

Secondly, based on the look-up table, the algorithm to achieve the decision for time frame n is illustrated in Algorithm 4. Note that in Algorithm 3, the CSI $\boldsymbol{H}(n)$ included in the involved expressions and problems (i.e., (19) ,(20), (22), (23) and (43)) should be replaced with the channel state $\boldsymbol{\chi}(n)$. On the other hand, in Algorithm 4, the actual CSI $\boldsymbol{H}(n)$ should be used when solving problem (22).

The computational complexity of Algorithm (4) originates mainly from solving problem (22) by Algorithm 2. Denote the computational complexity of the golden search method as c_1 and the computational complexity of solving problem (27) as c_2. Then, the computational complexity of achieving the decision for time frame n is $\mathcal{O}\{c_1(1 + c_2)\}$. Thus, Algorithm (4) can be implemented online in real time.

IV. OPTIMIZATION OF WIRELESS-POWERED RELAYING WITH FULL CSI

If full CSI is available, the transmitters of the source and the relay have prior knowledge of the fading CSI in N time frames over one finite time horizon at the beginning of the first time frame. This case provides an upper bound on the maximum throughput for any distribution of the fading channels. In this section, we investigate the optimization policy with full CSI to reveal the upper bound of throughput for the WPRN.

Algorithm 4 Optimization of the Decision With Causal CSI for Time Frame n

Acquire the actual CSI $\boldsymbol{H}(n)$ and calculate the corresponding quantized channel state $\boldsymbol{\chi}(n)$,
Acquire the battery energy state $B(n)$ and search for the entry corresponding to $\boldsymbol{\Gamma}(n)$,
Obtain $\phi^*(n)$ from the located entry.
if $\phi^*(n) = 0$ **then**
  The relay operates in EH mode.
else
  Obtain $\bar{B}^*(n+1)$ from the located entry and substitute $B(n+1) = \bar{B}^*(n+1)$ into problem (22),
  Solve problem (22) to achieve the decision and the relay operates in IR mode.
end if

A. PROBLEM FORMULATION AND DECOUPLING PROBLEM BY DYNAMIC PROGRAMMING

Given full CSI, $\boldsymbol{H}(n)$ is deterministic. Then, the throughput in the objective function in problem (6) can be expressed in a deterministic form. Thus, the throughput maximization problem for the same problem (6) is rewritten as

$$\max_{\pi \in \prod} \sum_{n=1}^{N} R(n) \quad \text{s.t. (5).} \tag{44}$$

By dynamic programming, problem (44) can be solved by proceeding backward in time from time frame N to time frame 1 to solve the following Bellman equations,

$$J^*(B(N), N) = \max_{\Omega(N)} \phi(N) R(N) \quad \text{s.t. (11),} \tag{45}$$

and

$$J^*(B(n), n) = \max_{\Omega'(n)} \phi(n) R(n) + J^*(B(n+1), (n+1)) \quad \text{s.t. (8),} \tag{46}$$

where $n \in \mathcal{N}^-$.

Clearly, the Bellman equations in (45) and (46) have structures similar to those in (12) and (13) for the optimization policy with causal CSI, except that $J^*(B(n+1), (n+1))$ is calculated in a deterministic form. Thus, based on the results derived for the optimization policy with causal CSI, we provide the solutions to the Bellman equations in (45) and (46) in the following two subsections.

B. OPTIMAL RELAY OPERATION MODE

For problem (45), we have the optimal $\phi^*(N) = 1$. For $n \in \mathcal{N}^-$, as a consequence of Theorem 1, the optimal $\phi^*(n)$ for problem (46) is stated in Corollary 1, whose proof is similar to that of Theorem 1.

Corollary 1: The optimal $\phi^*(n)$ for problem (46) can be obtained as

$$\phi^*(n) = \begin{cases} 0, & J_0^*(B(n), n) \geq J_1^*(B(n), n) \\ 1, & \text{otherwise}, \end{cases} \tag{47}$$

where

$$J_0^*(B(n), n) = J^*\left(\tilde{B}(n+1), (n+1)\right) \tag{48}$$

and

$$J_1^*(B(n), n) = \max_{\Omega''(n)} R(n) + J^*\left(B(n+1), (n+1)\right) \quad \text{s.t. (21b).} \tag{49}$$

C. OPTIMIZATION OF THE AUXILIARY ENERGY STATE AND THE RESOURCE ALLOCATION IN IR MODE

For $n = N$, according to (45), the optimization problem for the resource allocation in IR mode is the same as that in (43) for causal CSI. Thus, Algorithm 2 can be employed to optimize the resource allocation in IR mode.

For $n \in \mathcal{N}^-$, the optimization of resource allocation in IR mode can be achieved by solving problem (49). To achieve this goal, as in section III-E, problem (49) is decomposed into two subproblems for time frame n and time frame $(n+1)$. While the problem for time frame n is the same as problem (22), the problem for time frame $(n+1)$ is expressed as

$$J_1^*(B(n), n) = \max_{B(n+1)\in\mathcal{B}'} F^*(B(n+1)) + J^*\left(B(n+1), (n+1)\right). \tag{50}$$

Then, to obtain the solution to problem (49), we first solve problem (22) to obtain $F^*(B(n+1))$ by Algorithm 2 and then solve problem (50) by the exhaustive search method.

Based on the derived optimal relay operation mode and resource allocations in IR mode, the Bellman equations in (45) and (46) can be solved. Thus, the decision for each $B(n) \in \mathcal{B}$ $(n \in \mathcal{N})$ can be obtained. Based on the obtained decisions and $B(1)$, the optimization policy with full CSI can be achieved, and the corresponding algorithm is illustrated in Algorithm 5.

Algorithm 5 Algorithm to Obtain the Optimization Policy With Full CSI

1: Acquire $B(1)$ and $\boldsymbol{H}(n)$ $(n \in \mathcal{N})$ in N time frames over one finite time horizon and initialize $\mathcal{B}$.
2: **for** all possible $B(N) \in \mathcal{B}$ **do**
3: Let $\phi^*(N) = 1$, and employ Algorithm 2 to obtain the optimal $\bar{\Omega}^*(N)$ to problem (43).
4: Let $\Omega^*(N)|_{B(N)} = \Omega^*(N) = \phi^*(N) \bigcup \bar{\Omega}^*(N)$ and calculate $J^*(B(N), N)$.
5: **end for**
6: Set $n = N$.
7: **Repeat:**
8: Update $n = n - 1$.
9: **for** all possible $B(n) \in \mathcal{B}$ **do**
10: Calculate $J_0^*(B(n), n)$ by (48), solve problem (22) and (50) to obtain $\Omega''^*(n)$ and $J_1^*(B(n), n)$, and determine the optimal $\phi^*(n)$ by (47).
11: **if** $\phi^*(n) = 0$ **then**
12: Let $\Omega^*(n) = \{\phi^*(n)\}$ and $J^*(B(n), n) = J_0^*(B(n), n)$.
13: **else**
14: Let $J^*(B(n), n) = J_1^*(B(n), n)$ and obtain $\Omega^*(n)$ from $\Omega''^*(n)$.
15: **end if**
16: Let $\Omega^*(n)|_{B(n)} = \Omega^*(n)$.
17: **end for**
18: **Until:** $n = 1$.
19: Obtain the optimal π^* based on $\Omega^*(1)|_{B(1)}$.

V. NUMERICAL RESULTS

In the WPRN, the channels are assumed to be independent and identically distributed (i.i.d.) complex Gaussian distributions with zero mean and unit variance. The distances of the SR and RD links are denoted as d_{SR} and d_{RD}, respectively. For all results illustrated in the following, the distances are set to $d_{\mathrm{SD}} = 10$ m, $d_{\mathrm{SR}} = \kappa d_{\mathrm{SD}}$ and $d_{\mathrm{RD}} = d_{\mathrm{SD}} - d_{\mathrm{SR}}$. As in [34], the path-loss models of the SR and RD links are estimated as $\left(20 + 20\log_{10} d_{\mathbf{pq}}\right)$, where $d_{\mathbf{pq}}$ is the distance from node $\mathbf{p}$ to node $\mathbf{q}$. The antenna noise power and signal processing noise power are set to $\sigma_{\mathrm{a}}^2 = \sigma_{\mathrm{b}}^2 = -60$ dBm, and it is assumed that $\sigma_{\mathrm{R}}^2 = \sigma_{\mathrm{D}}^2 = \sigma_{\mathrm{a}}^2 + \sigma_{\mathrm{b}}^2$. The length of one time frame is set as $T = 0.5$ ms, the length of one finite time horizon is set to $N = 10$, and the energy conversion efficiency is set to $\tau = 0.8$. The battery energy states are discretized with step size $\frac{k_B E_0}{M}$, where $k_B = 2$, $M = 20$ and $E_0 = \eta P_{\mathrm{S}} T \overline{H}_{\mathrm{SR}}$ is the average energy harvested from the RF signals emitted by the source in one time frame, where $\overline{H}_{\mathrm{SR}}$ denotes the mean of H_{SR}. The initial battery energy state is set to $B(1) = 0$, and the number of finite states of the wireless channel gains is set to $K = 20$. In the following simulations, unless specified otherwise, the proposed scheme to be evaluated is the scheme with causal CSI that is implemented by Algorithm 4.

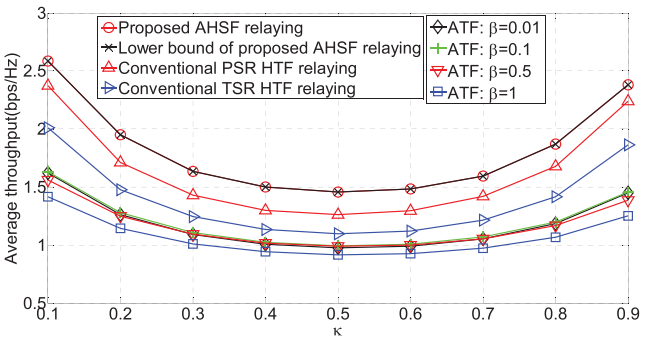

FIGURE 2. Average throughput as the relay position varies and $P_S = 20$ dBm. Comparison of the proposed AHSF relaying scheme with the HTF and ATF relaying schemes.

A. PERFORMANCE COMPARISONS OF DIFFERENT SCHEMES

Figure 2 and Figure 3 illustrate the average throughput achieved by different schemes when the relay position

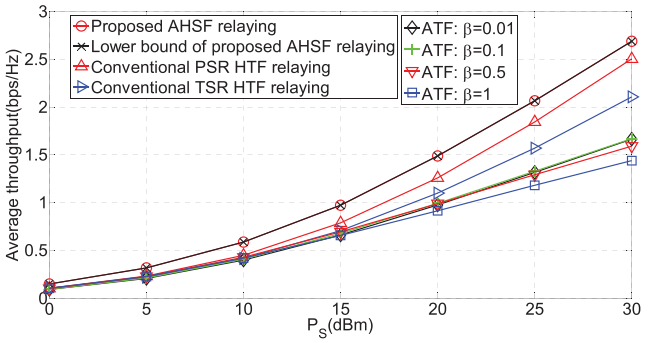

FIGURE 3. Average throughput as P_S varies and $\kappa = 0.5$. Comparison of the proposed AHSF relaying scheme with the HTF and ATF relaying schemes.

and P_S vary, respectively. The compared schemes are our proposed AHSF relaying scheme (denoted as "Proposed AHSF relaying" in the legend), the conventional PSR-based HTF relaying scheme (denoted as "Conventional HTF relaying") and four ATF relaying schemes, in which the preset fixed energy threshold is set as βE_0 (denoted as "ATF: $\beta = 0.01$", "ATF: $\beta = 0.1$", "ATF: $\beta = 0.5$' and 'ATF: $\beta = 1$"). Moreover, Figure 2 and Figure 3 illustrate the throughput calculated by the lower bound of the throughput achieved by the proposed AHSF relaying scheme when the noise power is not split by the PS receiver (denoted as "Lower bound of proposed AHSF relaying"). P_S is set to 20 dBm in Figure 2, and κ is set to 0.5 in Figure 3. Figure 2 and Figure 3 show that our proposed AHSF relaying scheme achieves significant throughput gains over the conventional HTF relaying scheme and the ATF relaying scheme. Specifically, the proposed scheme yields a maximum of 17% throughput gain over the HTF relaying scheme when $\kappa = 0.5$ in Figure 2 and a maximum of 45% throughput gain over the HTF relaying scheme when $P_S = 0$ dBm in Figure 3. Moreover, the throughput achieved by the ATF relaying scheme is much poorer than that achieved by our proposed relaying scheme and the conventional HTF relaying scheme since ATF relaying does not take the CSI into account. Finally, the throughput achieved by our proposed AHSF scheme is close to the lower bound, which indicates that the approximation by ignoring the split power of the noise does not have a substantial impact on the throughput performance.

B. COMPARISONS OF THE THROUGHPUTS WITH CAUSAL CSI AND FULL CSI

In Figure 4, we compare the average throughput achieved by the policy with causal CSI and that achieved by the policy with full CSI. The parameter settings in Figure 4 are the same as those in Figure 2. Figure 4 shows that the throughput achieved by the policy with causal CSI is approximately 95% of that achieved by the policy with full CSI. Therefore, by employing the practical policy with causal CSI in the WPRN, we can achieve throughput that is almost the same as the theoretical upper bound achieved by the optimization policy with full CSI.

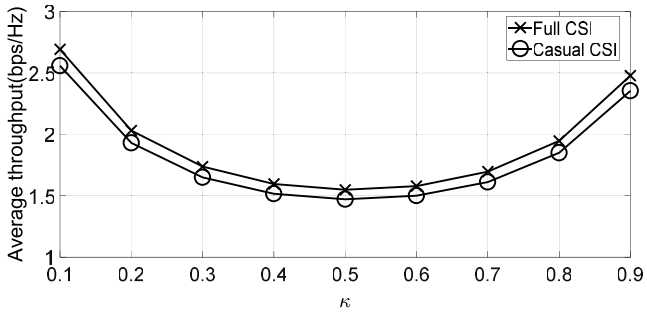

FIGURE 4. Comparison of the average throughput achieved by the policy with causal CSI and that achieved by the policy with full CSI.

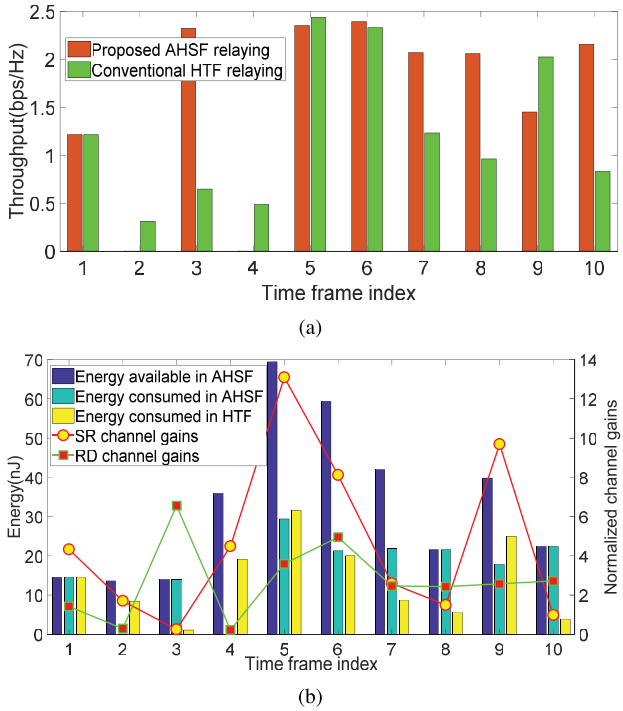

FIGURE 5. Snapshots of the throughput, energy and channel gains in a finite time horizon. (a) A snapshot of the throughput achieved by the proposed AHSF relaying scheme and the HTF relaying scheme in a finite time horizon. (b) A snapshot of the available energy and consumed energy in the proposed AHSF relaying scheme and the HTF relaying scheme and the channel gains in a finite time horizon.

C. ANALYSIS OF OPPORTUNISTIC EH AND IR IN THE AHSF RELAYING SCHEME

In Figure 5, we analyze how the relay performs EH and IR opportunistically in our proposed scheme by presenting snapshots of the throughput, battery energy states and channel gains over one finite time horizon. Here, we set $P_S = 20$ dBm and $\kappa = 0.5$. In Figure 5(a), we present a snapshot of the throughput achieved by the proposed AHSF scheme and the conventional HTF relaying scheme. In Figure 5(b), we present the available energy and consumed energy in the AHSF and HTF relaying schemes and the SR and RD channel gains. To facilitate observation, we normalize the channel gains as $\overline{\gamma} = \frac{\gamma}{10^5}$ in Figure 5(b), where γ refers to

$\gamma_{SR}(n)$ or $\gamma_{RD}(n)$. Note that for the conventional HTF relaying scheme, the relay always consumes all the available harvested energy to transmit; thus, the available energy is equal to the consumed energy.

Figure 5(b) shows that for the AHSF relaying scheme, the relay operates in EH mode in the 2nd and 4th time frames, where the RD channels are in deep fading and the SR gains are much larger than the RD channel gains. This scenario occurs because the consumed energy is zero in these time frames, so the relay performs EH opportunistically in these frames. Moreover, opportunistic EH also occurs in the 5th and 9th time frames, respectively, where the SR channel gains are much larger than the RD channel gains. The consumed energy in the AHSF relaying scheme is less than that in the HTF relaying scheme in these time frames, which indicates that the relay spends more resources on EH than on IR and reserves some energy for future usage in the AHSF relaying scheme. Meanwhile, in the 3rd time frame, where the RD channel gain is much larger than the SR channel gain, the relay transmits by consuming the energy harvested in the 2nd and 3rd time frame, which indicates that the relay performs IR opportunistically. Correspondingly, Figure 5(a) shows that the AHSF relaying scheme achieves much higher throughput than the conventional HTF relaying scheme in the 3rd time frame. Another example of opportunistic IR can be found in the 8th time frame, where the RD channel gain is larger than the SR channel gain, and the relay consumes all the available energy to transmit. The analyses for other time frames are omitted due to length limitations.

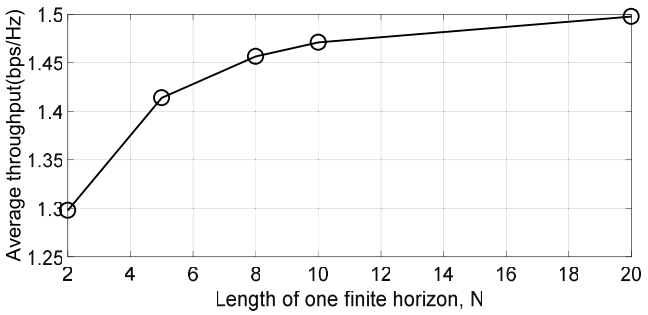

FIGURE 6. Average throughput as the length of one finite time horizon varies, where $\kappa = 0.5$ and $P_S = 20$ dBm.

D. IMPACT OF THE LENGTH OF ONE FINITE HORIZON ON THROUGHPUT PERFORMANCE

To evaluate the impact of the length of one finite time horizon on the throughput performance, the average throughput achieved by our proposed scheme with different values of N is illustrated in Figure 6. In this case, we set $\kappa = 0.5$ and $P_S = 20$ dBm. Figure 6 shows that the larger N is, the higher the throughput achieved because a larger N provides more wireless channel variations to be utilized in one finite time horizon. Furthermore, the achieved throughput increases sharply when N is small (e.g., N increases from 2 to 5) but increases slowly when N is large (e.g., N increases from 10 to 20). Nevertheless, the larger N is, the larger the size of the look-up table is, which increases the computational complexity of constructing the offline look-up table. Therefore, we need only a moderate value of N to achieve a trade-off between the throughput performance and the computational complexity of constructing the offline look-up table.

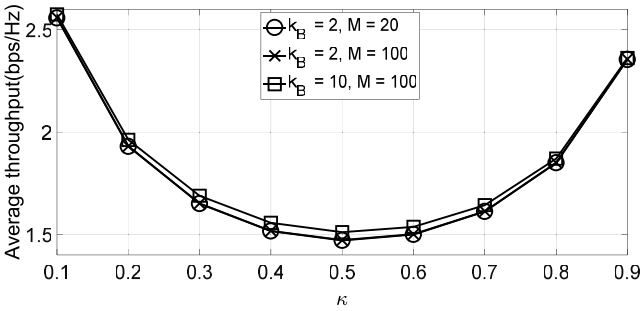

FIGURE 7. Average throughput achieved by the proposed scheme under different settings of B_s and M, where $P_S = 20$ dBm.

E. IMPACT OF B_s AND M ON THE THROUGHPUT PERFORMANCE

In the previous simulations, we set $B_s = k_B E_0$ with $k_B = 2$ and $M = 20$ for our proposed scheme. Since the amount of energy stored in the battery may be larger than $2E_0$, a lower bound of the throughput is obtained by setting $B_s = 2E_0$. Moreover, the larger M is, the more accurate the results and the higher the throughput that can be achieved. Therefore, setting $M = 20$ also results in a lower bound of the achieved throughput. To evaluate the impact of B_s and M on the throughput performance, we assess the average throughput achieved by our proposed scheme by setting $k_B = 10$ and $M = 100$ in Figure 7. In this case, we set $P_S = 20$ dBm. Figure 7 shows that when $k_B = 2$, the achieved throughput for $M = 20$ is almost the same as that for $M = 100$. This result indicates that for the value of B_s with $k_B = 2$, the throughput performance loss can be ignored by setting $M = 20$. Moreover, the throughput achieved for $k_B = 10$ and $M = 100$ is slightly higher than that for $k_B = 2$. Therefore, a larger B_s with a smaller quantized step can result in higher throughput, which also results in higher computational complexity. Nevertheless, the throughput lower bound achieved by setting $k_B = 2$ and $M = 20$ is similar to that obtained by setting k_B and M to larger values.

VI. CONCLUSIONS

In this paper, a new design with opportunistic EH and IR for the WPRN has been studied to improve the throughput. In presenting the new design, the AHSF protocol, which potentially enables the relay to perform EH and IR over one finite time horizon, has been proposed. Under the proposed protocol, a problem has been formulated to maximize the throughput by optimizing the relay operation mode and the resource allocation in IR mode in a finite time horizon. To address the time-coupled optimization problem,

an auxiliary battery energy state variable has been introduced, and dynamic programming has been employed to transform the problem into a series of Bellman equations. By solving the Bellman equations, an optimization policy with causal CSI has been proposed. Based on the derived results for the optimization policy with causal CSI, an optimization policy with full CSI has been further obtained to reveal the upper bound of throughput performance. Simulations have verified that our proposed scheme can achieve significant throughput gains over the existing HTF and ATF relaying schemes.

APPENDIX A
PROOF OF THEOREM 1

The optimal $\phi^*(n)$ can be obtained by comparing the optimal value of $J^*(\boldsymbol{s}(n), n)$ in (13) for $\phi(n) = 0$ with that for $\phi(n) = 1$.

When $\phi(n) = 0$, the value of equation (13) is expressed as $J_0^*(\boldsymbol{s}(n), n)$. By contrast, when $\phi(n) = 1$, the value of equation (13) is expressed as $J_1^*(\boldsymbol{s}(n), n)$. Thus, by comparing $J_0^*(\boldsymbol{s}(n), n)$ with $J_1^*(\boldsymbol{s}(n), n)$, we obtain the optimal $\phi^*(n)$, as illustrated in (19).

APPENDIX B
DERIVING $\lambda_{1,\min}$, $\lambda_{1,\max}$ AND $\upsilon_{1,\max}$

Since $\alpha_1(n) < \omega(n)$, from (33), we have $\frac{\upsilon_1(n)}{\lambda_1(n)G(n)} - \frac{1}{P_S\gamma_{\mathrm{SR}}(n)} \leq 1$, by which we can obtain

$$\lambda_1 \geq \frac{P_S\gamma_{\mathrm{SR}}(n)\upsilon_1(n)}{(1+P_S\gamma_{\mathrm{SR}}(n))G(n)} \triangleq \lambda_{1,\min}.$$

Meanwhile, from (32), we obtain

$$\begin{aligned}\lambda_1(n) &= \frac{\alpha_2(n)\upsilon_2(n)\gamma_{\mathrm{RD}}(n)}{\alpha_2(n)+\widetilde{p}_{\mathrm{R}}(n)\gamma_{\mathrm{RD}}(n)}\frac{1}{T} \\ &\leq \frac{(1-\upsilon_1(n))\gamma_{\mathrm{RD}}(n)}{T} \triangleq \lambda_{1,\max}.\end{aligned}$$

Clearly, $\lambda_{1,\max} \geq \lambda_{1,\min}$. Thus, we have

$$\frac{(1-\upsilon_1(n))\gamma_{\mathrm{RD}}(n)}{T} \geq \frac{P_S\gamma_{\mathrm{SR}}(n)\upsilon_1(n)}{(1+P_S\gamma_{\mathrm{SR}}(n))G(n)}.$$

Then, we obtain

$$\upsilon_1(n) \leq \frac{\zeta}{P_S\gamma_{\mathrm{SR}}(n)+\zeta} \triangleq \upsilon_{1,\max},$$

where $\zeta = (1+P_S\gamma_{\mathrm{SR}}(n))G(n)\gamma_{\mathrm{RD}}(n)/T$.

APPENDIX C
PROOF OF LEMMA 1

Lemma 1 can be proved by contradiction. Assume that the optimal solution $\Omega'''(n)$ satisfies that the left-hand side of (39) is less than the right-hand side. Then, $\alpha_2(n)$ can be reduced, as long as the right-hand side of (39) is no less than the left-hand side. Clearly, the constraint in (38b) is still satisfied when $\alpha_2(n)$ is reduced. Moreover, as $\alpha_2(n)$ decreases, the left-hand side of (39) increases since $\alpha_1(n) = 1-\alpha_2(n)$ increases, which results in an increasing value of the objective function. This result contradicts the assumption that the solution $\Omega'''(n)$ is optimal.

APPENDIX D
PROOF OF THEOREM 2

Theorem 2 can be proved by contradiction. Assume that the optimal solution $\Omega'''(n)$ satisfies that $T\alpha_2(n)p_{\mathrm{R}}(n) < B(n) - B(n+1)$. Then, $p_{\mathrm{R}}(n)$ can be increased until $T\alpha_2(n)p_{\mathrm{R}}(n) = B(n) - B(n+1)$ is satisfied. This causes the right-hand side of (39) to increase while the left-hand side does not decrease. According to Lemma 1, as the solution of $\Omega'''(n)$ is optimal, the objective function in (38a) is determined by the right-hand side of (39). Thus, the optimal value of the objective function in (38a) increases. This result contradicts the assumption that the solution $\Omega'''(n)$ is optimal.

REFERENCES

[1] M. Gastpar and M. Vetterli, "On the capacity of large Gaussian relay networks," *IEEE Trans. Inf. Theory*, vol. 51, no. 3, pp. 765–779, Mar. 2005.
[2] L. Fan, R. Zhao, F.-K. Gong, N. Yang, and G. K. Karagiannidis, "Secure multiple amplify-and-forward relaying over correlated fading channels," *IEEE Trans. Commun.*, vol. 65, no. 7, pp. 2811–2820, Jul. 2017.
[3] F. Zhou, L. Fan, X. Lei, G. Luo, H. Zhang, and J. Zhao, "Edge caching with transmission schedule for multiuser multirelay networks," *IEEE Commun. Lett.*, vol. 22, no. 4, pp. 776–779, Apr. 2018.
[4] J. Xu and R. Zhang, "Throughput optimal policies for energy harvesting wireless transmitters with non-ideal circuit power," *IEEE J. Sel. Areas Commun.*, vol. 32, no. 2, pp. 322–332, Feb. 2014.
[5] Y. Liang, H. Wu, G. Huang, J. Yang, and H. Wang, "Thermal performance and service life of vacuum insulation panels with aerogel composite cores," *Energy Buildings*, vol. 154, pp. 606–617, Nov. 2017.
[6] S. Gupta, R. Zhang, and L. Hanzo, "Energy harvesting aided device-to-device communication in the over-sailing heterogeneous two-tier downlink," *IEEE Access*, vol. 6, pp. 245–261, 2017.
[7] Z. Hu, C. Yuan, and F. Gao, "Maximizing harvested energy for full-duplex SWIPT system with power splitting," *IEEE Access*, vol. 5, pp. 24975–24987 , Oct. 2017.
[8] G. Zhang, J. Xu, Q. Wu, M. Cui, X. Li, and F. Lin, "Wireless powered cooperative jamming for secure OFDM system," *IEEE Trans. Veh. Technol.*, vol. 67, no. 2, pp. 1331–1346, Feb. 2018.
[9] Q. Li, Q. Zhang, and J. Qin, "Secure relay beamforming for SWIPT in amplify-and-forward two-way relay networks," *IEEE Trans. Veh. Technol.*, vol. 65, no. 11, pp. 9006–9019, Nov. 2016.
[10] A. A. Nasir, X. Zhou, S. Durrani, and R. A. Kennedy, "Relaying protocols for wireless energy harvesting and information processing," *IEEE Trans. Wireless Commun.*, vol. 12, no. 7, pp. 3622–3636, Jul. 2013.
[11] Y. Shen, X. Huang, K. S. Kwak, B. Yang, and S. Wang, "Subcarrier-pairing-based resource optimization for OFDM wireless powered relay transmissions with time switching scheme," *IEEE Trans. Signal Process.*, vol. 65, no. 5, pp. 1130–1145, Mar. 2017.
[12] G. Huang, Q. Zhang, and J. Qin, "Joint time switching and power allocation for multicarrier decode-and-forward relay networks with SWIPT," *IEEE Signal Process. Lett.*, vol. 22, no. 12, pp. 2284–2288, Dec. 2015.
[13] G. Huang and D. Tang, "Wireless information and power transfer in two-way OFDM amplify-and-forward relay networks," *IEEE Commun. Lett.*, vol. 20, no. 8, pp. 1563–1566, Aug. 2016.
[14] G. Huang and W. Tu, "Joint power splitting and power allocation for two-way OFDM relay networks with SWIPT," *Comput. Commun.*, vol. 124, pp. 76–86, Jun. 2018.
[15] Y. Huang, J. Wang, P. Zhang, and Q. Wu, "Performance analysis of energy harvesting multi-antenna relay networks with different antenna selection schemes," *IEEE Access*, vol. 6, pp. 5654–5665, 2018.
[16] Z. Zhou, M. Peng, Z. Zhao, and Y. Li, "Joint power splitting and antenna selection in energy harvesting relay channels," *IEEE Signal Process. Lett.*, vol. 22, no. 7, pp. 823–827, Nov. 2014.
[17] J. L. Zhang and G. F. Pan, "Outage analysis of wireless-powered relaying MIMO systems with non-linear energy harvesters and imperfect CSI," *IEEE Access*, vol. 4, pp. 7046–7053, 2016.
[18] X. Wang, J. Liu, and C. Zhai, "Wireless power transfer-based multi-pair two-way relaying with massive antennas," *IEEE Trans. Wireless Commun.*, vol. 16, no. 11, pp. 7672–7684, Nov. 2017.

[19] G. Amarasuriya, E. G. Larsson, and H. V. Poor, "Wireless information and power transfer in multiway massive MIMO relay networks," *IEEE Trans. Wireless Commun.*, vol. 15, no. 6, pp. 3837–3855, Jun. 2016.
[20] Y. Feng, V. C. M. Leung, and F. Ji, "Performance study for SWIPT cooperative communication systems in shadowed Nakagami fading channels," *IEEE Trans. Wireless Commun.*, vol. 17, no. 2, pp. 1199–1211, Feb. 2018.
[21] Y. Xu *et al.*, "Joint beamforming and power-splitting control in downlink cooperative SWIPT NOMA systems," *IEEE Trans. Signal Process.*, vol. 65, no. 18, pp. 4874–4886, Sep. 2017.
[22] Y. Zhang, J. Ge, and E. Serpedin, "Performance analysis of a 5G energy-constrained downlink relaying network with non-orthogonal multiple access," *IEEE Trans. Wireless Commun.*, vol. 16, no. 12, pp. 8333–8346, Dec. 2017.
[23] X. F. Di, K. Xiong, P. Y. Fan, and H.-C. Yang, "Simultaneous wireless information and power transfer in cooperative relay networks with rateless codes," *IEEE Trans. Veh. Technol.*, vol. 66, no. 4, pp. 2981–2996, Apr. 2017.
[24] J. Qiao, H. Zhang, X. Zhou, and D. Yuan, "Joint beamforming and time switching design for secrecy rate maximization in wireless-powered FD relay systems," *IEEE Trans. Veh. Technol.*, vol. 67, no. 1, pp. 567–579, Jan. 2018.
[25] B. Li, Z. Fei, and H. Chen, "Robust artificial noise-aided secure beamforming in wireless-powered non-regenerative relay networks," *IEEE Access*, vol. 4, pp. 7921–7929, Nov. 2016.
[26] C. Yin, H. T. Nguyen, C. Kundu, Z. Kaleem, E. Garcia-Palacios, and T. Q. Duong, "Secure energy harvesting relay networks with unreliable backhaul connections," *IEEE Access*, vol. 6, pp. 12074–12084, May 2018.
[27] Z. Zhou, M. Peng, Z. Zhao, W. Wang, and R. S. Blum, "Wireless-powered cooperative communications: Power-splitting relaying with energy accumulation," *IEEE J. Sel. Areas Commun.*, vol. 34, no. 4, pp. 969–982, Apr. 2016.
[28] A. A. Nasir, X. Zhou, S. Durrani, and R. A. Kennedy, "Wireless-powered relays in cooperative communications: Time-switching relaying protocols and throughput analysis," *IEEE Trans. Commun.*, vol. 63, no. 5, pp. 1607–1622, May 2015.
[29] Y. Gu, H. Chen, Y. Li, and B. Vucetic, "Wireless-powered two-way relaying with power splitting-based energy accumulation," in *Proc. IEEE Global Commun. Conf. (GLOBECOM)*, Dec. 2017, pp. 1–6.
[30] Z. Li, H. Chen, Y. Li, and B. Vucetic, "Incremental accumulate-then-forward relaying in wireless energy harvesting cooperative networks," in *Proc. IEEE Global Commun. Conf. (GLOBECOM)*, Dec. 2017, pp. 1–6.
[31] Y. Gu, H. Chen, Y. Li, Y. C. Liang, and B. Vucetic, "Distributed multi-relay selection in accumulate-then-forward energy harvesting relay networks," *IEEE Trans. Green Commun. Netw.*, vol. 2, no. 1, pp. 74–86, Mar. 2018.
[32] K.-H. Liu, "Performance analysis of relay selection for cooperative relays based on wireless power transfer with finite energy storage," *IEEE Trans. Veh. Technol.*, vol. 65, no. 7, pp. 5110–5121, Jul. 2016.
[33] A. Host-Madsen and J. Zhang, "Capacity bounds and power allocation for wireless relay channels," *IEEE Trans. Inf. Theory*, vol. 51, no. 6, pp. 2020–2040, Jun. 2005.
[34] X. Zhou, R. Zhang, and C. K. Ho, "Wireless information and power transfer: Architecture design and rate-energy tradeoff," *IEEE Trans. Commun.*, vol. 61, no. 11, pp. 4754–4767, Nov. 2013.
[35] W. J. Huang, Y. W. P. Hong, and C. C. J. Kuo, "Lifetime maximization for amplify-and-forward cooperative networks," *IEEE Trans. Wireless Commun.*, vol. 7, no. 5, pp. 1800–1805, May 2008.
[36] P. Sadeghi, R. A. Kennedy, P. B. Rapajic, and R. Shams, "Finite-state Markov modeling of fading channels—A survey of principles and applications," *IEEE Signal Process. Mag.*, vol. 25, no. 5, pp. 57–80, Sep. 2008.
[37] Z. Ding, S. M. Perlaza, I. Esnaola, and H. V. Poor, "Power allocation strategies in energy harvesting wireless cooperative networks," *IEEE Trans. Wireless Commun.*, vol. 13, no. 2, pp. 846–860, Feb. 2014.
[38] D. P. Bertsekas, *Dynamic Programming and Optimal Control*, vol. 1. Belmont, MA, USA: Athena Scientific, 1995.
[39] S. Boyd and L. Vandenberghe, *Convex Optimization*. Cambridge, U.K.: Cambridge Univ. Press, 2004.
[40] M. Grant and S. Boyd. (Sep. 2013). *CVX: Matlab Software for Disciplined Convex Programming, Version 2.0 Beta*. [Online]. Available: http://cvxr.com/cvx

GAOFEI HUANG received the M.S. and Ph.D. degrees from Sun Yat-sen University, China, in 2004 and 2012, respectively. He is currently a Lecturer with Guangzhou University, China. His current research interests include energy-harvesting wireless communication networks, and the resource allocation in next-generation wireless communication systems and cross-layer design of wireless communication systems.

WANQING TU received the Ph.D. degree from the Department of Computer Science, City University of Hong Kong. She is currently a Senior Lecturer with the Department of Computing Science, The University of Auckland, New Zealand. Her research interests include wireless multi-hop communications, multimedia communications, QoS/QoE, IoT, overlay networks, and distributed computing. She received an IRCSET Embark Initiative Post-Doctoral Research Fellowship, and the Best Paper Award in 2005.